INTERNATIONAL JOURNAL OF MARITIME TECHNOLOGY
IJMT Vol.8/ Summer 2017 (25-34)

Available online at: http://ijmt.ir/browse.php?a_code=A-10-891-1&sid=1&slc_lang=en

Investigation of Drag Coefficient at Subcritical and Critical Reynolds Number Region for Circular Cylinder with Helical Grooves

Md. Ashraful Haque[1], Abdur Rauf[1], Dewan Hasan Ahmed[1*]

[1] Department of Mechanical and Production Engineering, Ahsanullah University of Science and Technology,141-142 Love Road, Tejgaon Industrial Area, Dhaka, Bangladesh; dhahmed.mpe@aust.edu

ARTICLE INFO

Article History:
Received: 1 Jul. 2017
Accepted: 12 Oct. 2017

Keywords:
Helical groove
circular cylinder
drag coefficient
subcritical Reynolds number
critical Reynolds number
drag force

ABSTRACT

Drag reduction of an object is the major concern in many engineering applications. Experimental studies have been carried out on circular cylinder with helical grooves in a subsonic wind tunnel. Different cases of helical grooves with different pitches, helical groove angles and number of starts of helical groove on circular cylinder are tested. Experimental results show the drag coefficient is sensitive with Reynolds number and decreases at critical Reynolds number and at subcritical and supercritical or transcritical Reynolds number the drag coefficient increases as compared with smooth cylinder. The longitudinal grooves over the cylinder surface are tested and showed that drag coefficient much decreases at the subcritical and critical Reynolds number region. The experimental results are validated with available literature and obtained good agreement.

1. Introduction

In recent years, many industries including automobile sectors are giving much importance on fuel economy of vehicle, stabilization of the object etc. For example, lower value of drag is the common goal to achieve in different applications. Efforts are continued for ships, submarine, aviation and other related industries also. There are various ways improve the fuel economy of the vehicle or stabilizing the structures. However, efforts on aerodynamics or drag reduction are put ahead to concern the above issues by the researchers around the world. In fact, reduction of drag coefficient is comparatively easy way to have fuel economical vehicle, stabilizing the chimney, tower, building, hydraulic structure etc. The phenomenon of drag can be simulated and measured by recreating air flow over an object. Drag co-efficient (CD) is not constant but varies as a function of speed, angle of attack, object position, object size, fluid density and fluid viscosity etc. Flow around a circular cylinder was intensively studied in the past and that returns to its simple geometry as well as the logical structure of the vortices. The studies were led on the one hand by academic interest and on the other hand by practical interest (industrial).There are two types of method to reduce drag force of a cylinder i.e. active and passive control. The active control methods order the flow by ensuring external energy by means such as the acoustic excitation or the jet blow. The passive control methods order the flow by modifying the shape of the body or by attaching additives devices such as elements of roughness on the body Sakamoto et al. [1], Fujisawa and Takeda [2].

Many studies about passive control techniques exist to reduce the drag forces, for example, Igarashi and Tsutsui [3, 4], who have installed a tip-wire in the separate shearing layer of a cylinder for a Reynolds number Re = 4.2×10^4 and reduced the mean drag force acting on the cylinder by 20–30%, where the greatest reduction of drag is being obtained when a tip-wire was located under an angle of 120° at the stagnation point. It is well-known that the drag in a cylinder decreases when the wake behind it changes laminar flow with turbulent including a narrow wake width. Raayai-Ardakani and McKinley [5] includes wrinkled surface and show that the surface texture can be able to reduce the skin friction drag. Massumoto et al. [6] proposed apple shape geometry and compared with sphere and different hollow shaped geometries like U-shaped, V-shaped grooves and find that apple shape geometry can reduce the drag up to 23% as compared with sphere and 13% with circular cylinder. In recent time Yunging et al. [7] reviewed the different drag reduction mechanism and importance of drag reduction in different applications. Among these groove surface plays vital role on drug reduction along with coating and other issues.

Zdravkovich [8] suggested a method for reducing drag by using an obstacle placed upstream or downstream to alter the flow field around the bluff body. Sakamoto

and Haniu [9] studied the suppression of the fluid forces acting on a cylinder when a control rod was added to the system. They remarked that the time-averaged mean drag force could be reduced until approximately to 50%, and that the drag forces could be reduced up to 85% by using a control rod. Strakes or grooves on the cylinder surfaces are the also investigated by many researchers to reduce the drag coefficient and observe the flow behavior over cylinder surface and continued to the downstream by analyzing the vortices, separation etc. Bai et al. [10] carried out numerical study on four different surface textures like V-shaped, saw tooth, rectangular, and semi-circular sections. They observed that the peak of v-shaped groove causes the secondary vortex which influence the near wall flow region. Coustols [11] has studied the effect of the grooved walls on the structure of a turbulent boundary layer, he has tested a various forms of grooves as triangular in "V", in the form of "U" and also in the form of "L". In these three kinds of grooves, he noted that the "L" form had reduced the drag about 10%. The idea to make grooves on the cylinder is also from a study made by Talley and Mungal [12] they noticed that the plants of cactus have a strong resistance against the wind forces and that returns to their longitudinal grooves.

Yokoi et al. [13] carried out experiments on grooved cylinders and they found that the drag effect with lower number of grooves on circular cylinder is negligible when the angle of attack varies. However, as long as the number of grooves increases over the cylinder surface, the drag coefficient is independent on the angle of attack. On other hand, Yamagishi and Oki [14] observed that the separation point has shifted further downstream position when the cylinder surface is in grooved pattern and the position of reattachment is located near the maximum pressure region. However, they have found the critical Reynolds number is much less as compared with the smooth cylinder surface and drag coefficient is decreased for that particular Reynolds number. Takayama and Aoki [15] showed that the grooved surface over the circular cylinder and the groove depth influence the drag coefficient and critical Reynolds number decreases for higher depth of the groove. Dey and Das [16] carried out numerical investigation on extended solid over the circular cylinder surface and observed that lift and drag can be reduced and influenced by the length of the extended surface. However, their investigation was for low Reynolds number.

Ranjith et al. [17] carried out numerical analysis on drag coefficient on circular cylinder with helical strakes. They imposed three starts helical strakes over the cylinder surface and found that the drag coefficient increases as compared with the smooth cylinder. However, they conducted the numerical investigation only for two Reynolds number like 100 and 28000. They claimed that the helical strake regulates the separation and interact at a farther distance at the downstream than the bare cylinder. Similarly Quen et al. [18] also went through the experimental study and observed that helical strake doesn't benefit to the drag coefficient. However, Shaun [19] found that the drag coefficient can be reduced up to 25% at the sub-critical Reynolds number region with the three start helical groove while they were conducting their experiments in towing tank.

The present study tries to investigate the helical groove with different starts and pitches over the circular cylinder surface on drag coefficient over a wide range of Reynolds numbers.

2. Experimental set up:

The experiments were carried out at 30cm × 30cm × 60cm (w×h×l) open circuit subsonic wind tunnel of Model AF100 of TecQuipment with a wide range wind velocity. At first a smooth cylinder was tested. Then the experiments were carried out for different orientation of helical grooves and longitudinal grooves on circular cylinder. All the cylinders have main dimensions as follows:

- Length L: 24.8 ± 0.5 cm (25cm used for data calculation)
- Diameter D: 8.38 ± 0.5 cm (8.5cm used for data calculation)
- In grooved cylinders, the groove has rectangular cross section with the width 0.4cm and the depth 0.2cm.
- Groove depth (H) to test cylinder diameter (D) ratio was H/D = 2.4%. Cylinder length to diameter ratio was A/R=2.9 (aspect ratio).

The smooth cylinder is a PVC hollow circular cylinder with PVC carpet (polyvinyl chloride) wrapped on its surface using glue. The two open end of the cylinder closed by two circular cock-sheet having equivalent diameter of cylinder. The experimental setup and the placement of the object in wind tunnel are shown in Figure 1.

The drag force on cylinder measured with Three-Component Balance (AFA3). A supporting rod adjusted to the three component balance at one side through side wall. Cylinder fixed with free end of the supporting rod through longitudinal axis. Cylinders were tested at the center of the flow and also at the center of the test section as shown in Figure 1. Cylinders ends are free from side walls of the test section. Separate control and instrumentation unit

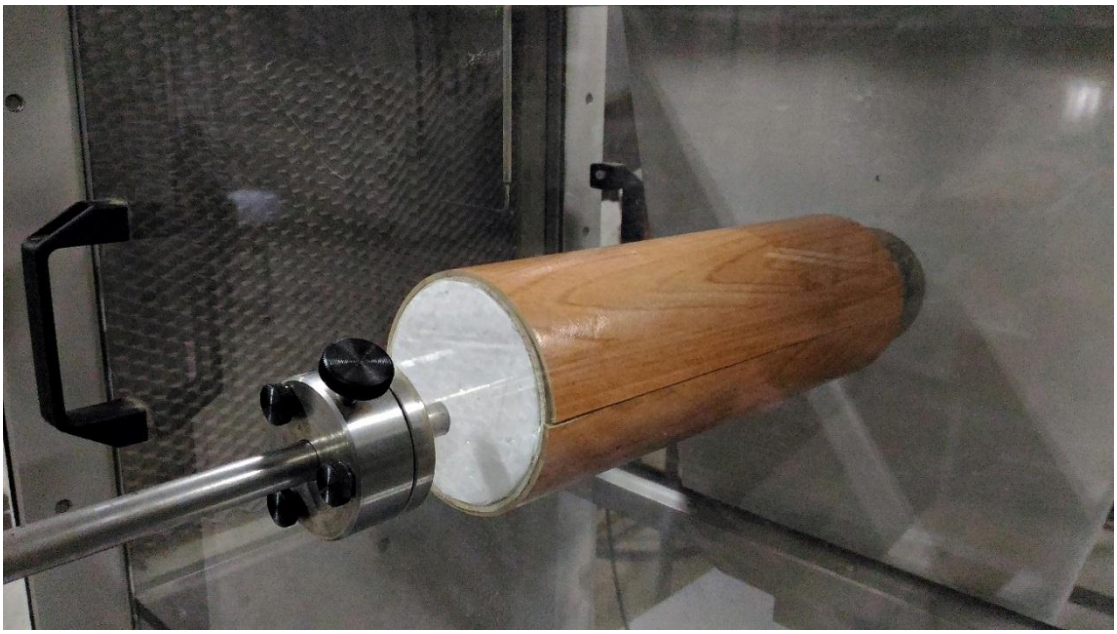

Figure 1. Experimental setup and object orientation in the wind tunnel.

controls the speed of the axial fan, hence, air velocity in the test section of the wind tunnel. The air pressure was measured by Tube Manometer (AFA1) and the velocity of air calculated from the pressure difference with the following equation:

$$V = \sqrt{\frac{2\Delta P}{\rho}}$$

where Δp = pressure difference of the pitot static tube at the free stream region of the wind tunnel and ρ = density.

Dynamic pressure is calculated as $q_\alpha = \frac{1}{2}\rho V^2$

Therefore, the drag coefficient, $C_D = \frac{F}{q_\alpha A}$

where A is the projection area, which is equal to the multiplication of length and diameter of the tested cylinder.

3. Results and Discussions

Before, conducting the experiments on grooved surface of the test cylinder, a smooth test cylinder is taken into account to verify the drag coefficient over a range of Reynolds number especially at the critical Reynolds number region. Figure 2 shows the drag coefficient for different Reynolds number for the test cylinder. The results show the similar trend of drag co-efficient as a function of Reynolds number as found in literature. There is some deviation of the present study with the smooth surface of the cylinder. This may be due to the wrapping of the PVC floor plastic carpet when the two edges may not aligned and match at the same line along

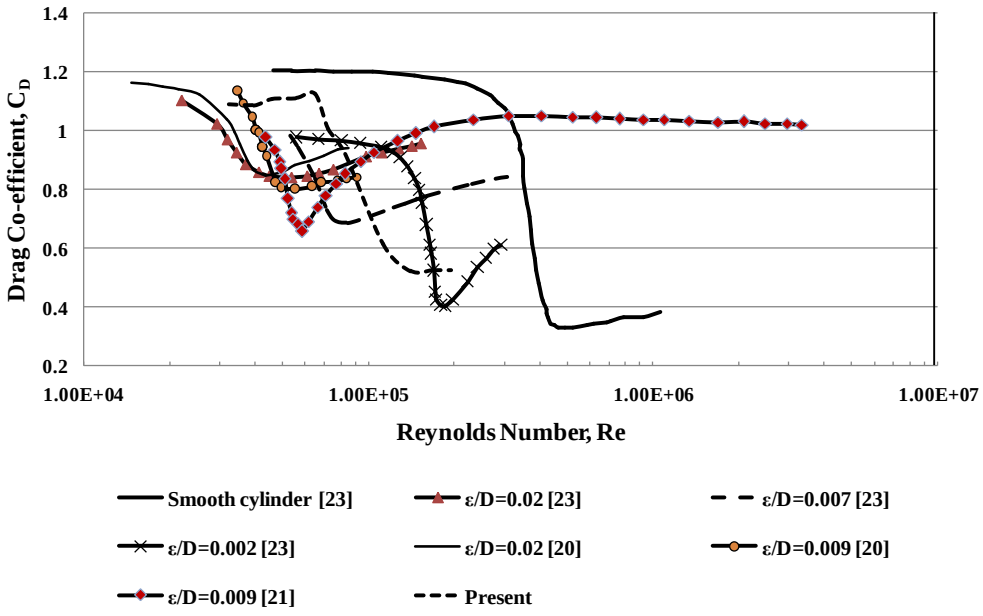

Figure 2. Validation of the drag co-efficient against Reynolds number with available literature.

the longitudinal axis. In addition, the test cylinder's surface was not rigid; in fact, the surface was smooth enough as it was wrapped by Polyvinyl chloride (PVC) floor plastic carpet. However, there are much deviations of drag coefficient for different effective roughness in the literature. For example, ε/D = 0.009, the drag co-efficient profile much varied for Fage and Warsap [20] and Achenbach [21]. Little variation of effective roughness (from 0.009 to 0.007) also makes significant variation of the drag co-efficient profile. Adachi [22] explained that the critical Reynolds number decreases with the increase of the roughness. Hojo [23] also found similar findings on drag coefficient. Moreover, the aspect ratio of reference curves are infinite where aspect ratio for the cylinders of present study are very small (L/D=2.9). However, present study shows reasonable trend for the drag co-efficient profile.

Experiments with helical grooves:

The helical grooves are created on circular cylinder by cutting PVC carpet with appropriate size and shape and placing it on the surface of the cylinder using glue. Two open ends of the cylinder are closed by circular cock-sheet as before. Experiments are conducted on the cylinders by varying different design parameter and detail of the case studies are shown in Table 1.

Table 1. Different case studies

Case study	Test cylinder	No. of start	Helical groove angle	Pitch
Case 1	Cylinder 1	Single	15º	Different pitches
	Cylinder 2	Single	30º	
	Cylinder 3	Single	45º	
	Cylinder 4	Single	60º	
Case 2	Cylinder 1	Single	15º	Same pitch (7cm)
	Cylinder 2	Double	28.18º	
	Cylinder 3	Triple	38.80º	
	Cylinder 4	Hex (six)	58.12º	
Case 3	Cylinder 1	Single	30º	Different pitches
	Cylinder 2	Two	30º	
	Cylinder 3	Single	60º	
	Cylinder 4	Hex (six)	60º	

Variation of helix-angle for single start helical groove:

With the validation of drag co-efficient of the bare cylinder, studies have been continued for numbers of experiment with four different helical groove angles with single start. The helical groove angles like 15º, 30º, 45º and 60º are constructed over the PVC floor plastic carpet. The designed grooves over the cylinder for different groove angles and the constructed cylinder with helical grooves are shown in Figure 3 and 4 respectively.

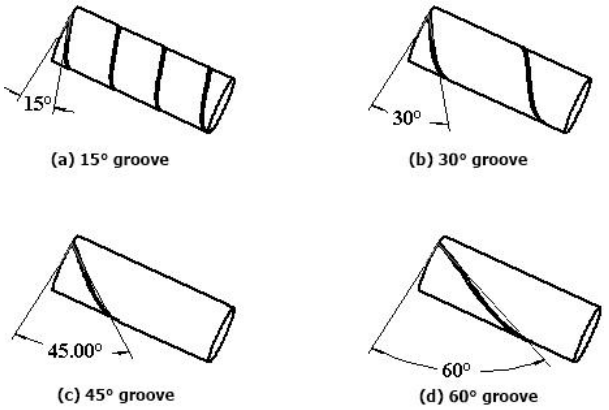

Figure 3. single start helical groove cylinder with (a) 15°, (b) 30°, (c) 45° and (d) 60° helix angle is measured with the transverse direction of the cylinder.

Figure 4. Smooth cylinder and groove cylinder of helix angle 15º, 30º, 45º and 60º respectively from left.

Experiments are carried with the same procedure as explained before. The calculated drag co-efficient for different groove angles over a range of Reynolds number are shown in Figure 5. The results show that groove angle influences the drag co-efficient, especially, for low Reynolds number lower groove angle (e.g. 15º groove angle) has lower drag co-efficient value, however, for higher groove angle exhibits lower drag co-efficient for higher Reynolds number. 15o helical groove angle means also the same angle with the free stream velocity. Therefore, increasing the groove angle results in moving grooved from the transverse direction to longitudinal direction or becoming the across the flow of the fluid direction.

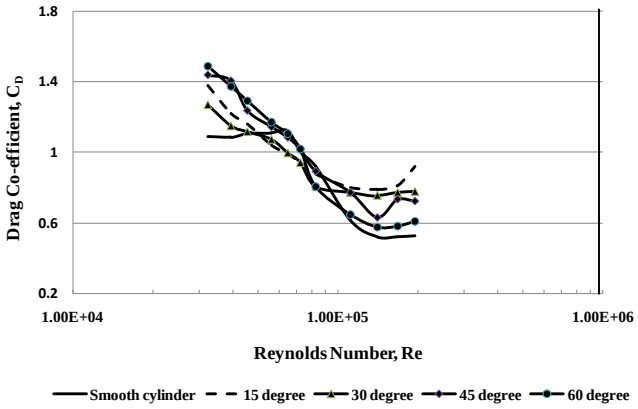

Figure 5- Variation of drag-coefficient as a function of Reynolds number for different helix-angle of single start helical groove.

Comparing the drag co-efficient with smooth surface of the test cylinder, smooth surface poses the low drag co-efficient except the critical Reynolds number region. However, to get the insight of the influence of the groove angles, the drag force variation over the Reynolds number is shown in Figure 6. The results show the drag forces are gradually decreases for higher groove angles.

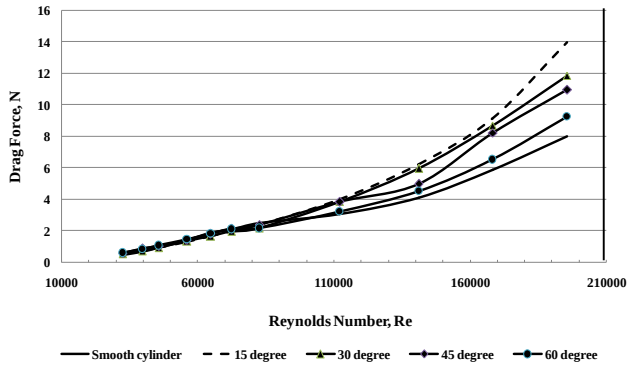

Figure 6. Variation of drag force as a function of Reynolds number for different helix-angle of single start helical groove.

Interestingly, the drag coefficient for grooved surface gradually decreases to its minimum value and then increases i.e. at super critical region. In fact, at the sub-critical Reynolds number region the drag coefficient with a grooved surface on cylinder is disappeared (as compare with smooth cylinder). The explanation can be made in the following ways. A separation point is usually found over the circular cylinder during the fluid flow even with the low Reynolds number. However, this separation point moves downstream of the cylinder surface with the increase of the Reynolds number. Rodriguez et al. [24] mentioned that the separation angle measuring from the front stagnation point varies from 91.5^o to 148^o during the critical to supercritical Reynolds number when the fluid flows over circular cylinder. However, for subcritical region the separation point may start from as below as 82^o [25]. Separation occurs at the leading edge and reattachment of fluid usually happens at trailing edge or some other point inside the groove [26] when the fluid passes over the groove. Helical grooves over the periphery of the cylinder covers all 360^o over a pitch length. Table 2 shows little glimpse of the pitch and predicted length of separation zone along the cylinder for critical Reynolds number region. Increasing the helical groove angle means the increase of the pitch and on other hand, lower helical groove angles leads to have smaller pitch but the number of pitch over the cylinder length increases. Figure 7 shows the different geometrical features of grooved surface on a circular cylinder. For example, ‘a, denotes the longitudinal distance for the fluid to pass over the groove for different groove angle. Groove angle with zero degree should have the value of ‘a’ is zero. Increasing the groove angle increases the value of ‘a’. The notation ‘b’ denotes the distance for the fluid to flow across the valley of the groove and for longitudinal groove the value of ‘b’ should be the width of the groove. Therefore, the value of b will decrease with the increase of ‘a’. This particular value of ‘a’ and ‘b’ reflects that the increase of the groove angle leads the fluid to flow to a far distance to cross the groove. Moreover, lower groove angle causes the increase of number of pitches over the cylinder length and ensures that much portion of the grooved surface at the frontal area of the cylinder surface (i.e. to the separation point). The grooved portion on the cylinder surface reduces at the upstream side (say upto the separation point) decreases with the increase of the groove angle.

Considering the subcritical Reynolds number when the Reynolds number is low and the fluid boundary layer is laminar and the separation of the fluid occurs much earlier [27]. For low helical groove angle the grooves are more inclined to the flow direction therefore, the separation which is enforced at the leading edge of the groove and continued to the far distance i.e. upto the tailing edge of the grooves. The gap between the leading and trailing edge (i.e. the point of separation and reattachment) is lower for higher helical groove angle. Therefore, the secondary separation point is bit earlier for higher groove angle than that of the lower helical groove angle and makes significant contribution on drag coefficient. In fact, with the presence of helical groove, fluid separation and attachment on the groove surface much earlier than the usual separation angle (say 82^o). This leads to have higher drag coefficient of the grooved surface than the smooth cylinder. Similar findings are also observed by Garcia et al. [28] and reported that valley and tip of a groove make contribution to shift the separation angle. It is also evident from the Figure 5 is that the increases the groove angle increases the drag coefficient.

Table 2. Geometrical feature with the change of helical groove

Groove Angle, (deg)	Pitch	Pitch/Length	Separation zone along the pitch (91.5^o to 148^o)	Number of starts
15	7.170551	0.28682	1.125378	1 start
30	15.42838	0.61714	2.421398	1 start
45	26.71126	1.06845	4.192184	1 start
60	46.25679	1.85027	7.259746	1 start
28.18	14.31785	0.28636	2.247108	2 starts
38.8	21.47923	0.28639	3.371045	3 starts
58.12	42.93966	0.28626	6.739142	6 starts

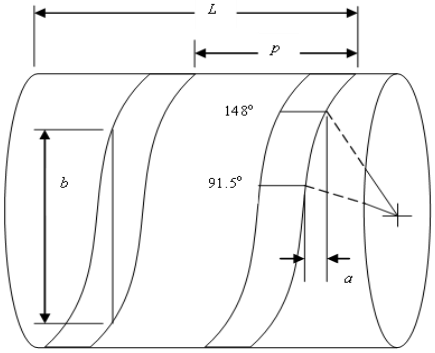

Figure 7. different geometrical features of grooved surface on a circular cylinder

The other issue which is related here that for certain helical groove angle the air/fluid is guided to flow in the groove channel. For example, with the longitudinal groove along the cylinder surface, the air crosses the valley where the separation and reattachment occurs with minimum distance. However, with a certain helical groove angle a portion of fluid is enforced to move along the groove channel. This movement of air along the groove channel makes a disturbance for air at downstream position of the cylinder surface. This disturbance of the fluid over the surface causes to have vortices at the downstream position of the groove and leads to create a wake; therefore, it is believed that the drag coefficient of the grooved surface is higher than the smooth surface. Notable finding from the figure is that the drag coefficient with helical groove at the sub-critical Reynolds number region gradually decreases rather than being straight (steady) for smooth cylinder.

The trend of decreasing of the drag coefficient of the circular cylinder with helical grooves is continued as long as Reynolds number increases till the critical Reynolds number. Increasing the value of Reynolds number (immediate after the subcritical Reynolds number) drags the boundary layer to further downstream position on the cylinder surface and causes to reduce the size of the wake and hence decreases the drag coefficient. It is reported that the range of the separation angle for critical Reynolds number region varies from 91.5^o to 148^o [24] which makes 1/7th of the longitudinal length of the pitch (see Table 2) of the present cylinder dimension. The separation at the leading edge of the groove and the reattachment at the trailing edge cause the separation at the late stage for higher Reynolds number. However, with the higher Reynolds number the turbulent boundary layer transition happens which extend the separation point further downstream position and causes to lower drag coefficient as compared with the smooth cylinder.

It can easily be observed that there is an early transition of critical Reynolds number region to supercritical number region for the grooved cylinder. These findings are consistent with Nakamura and Tomonari [29] and they explained that the rough strips/patterns at certain angular position near the separation region causes an early transition of critical Reynolds number region to supercritical Reynolds number. Ko et al. [30] also make similar agreement and extended their opinion also on transition from subcritical to critical Reynolds number region for the presence of groove on cylinder surface.

Actually, at low Reynolds number region for the smooth cylinder, the form drag which is contributed by the pressure dominates over the skin friction drag (contributed by shear stress). However, with the increase of the roughness both drag contributes significantly for the total drag. Considering the critical Reynolds number region, the grooved cylinder surface poses lower drag coefficient which implies that the pressure drag reduced significantly. In addition, at the groove the pressure becomes higher as compared with the cylinder surface. In fact, at the front edge of the groove there is a flow separation and it reattach somewhere at the end edge of the groove. With this consequence, wall shear stress reduces at the front edge of the groove leads to separate the boundary layer and leads to have lower pressure drag. However, for turbulent flow, separation of the turbulent boundary layer becomes difficult.

Same pitch with different number of starts:

Experiments are continued for the different arrangement of grooves. In this particular case, the pitch of the helical groove over the cylinder surface is kept same as 7 cm. Helical groove angle and number of the starts are varied over the cylinder surface to maintain the same pitch. Therefore, the helical groove angle changes to 15^o, 28^o, 45^o and 58^o with the number of starts as 1, 2, 3 and 6 respectively. The schematic diagrams for the helical grooves over the cylinder surface with same pitch are shown in Figure 8. The calculated drag co-efficient results show (see Figure 9) that the smooth surface cylinder exhibits lower drag co-efficient than the grooved surface for the same pitch at low Reynolds number region.

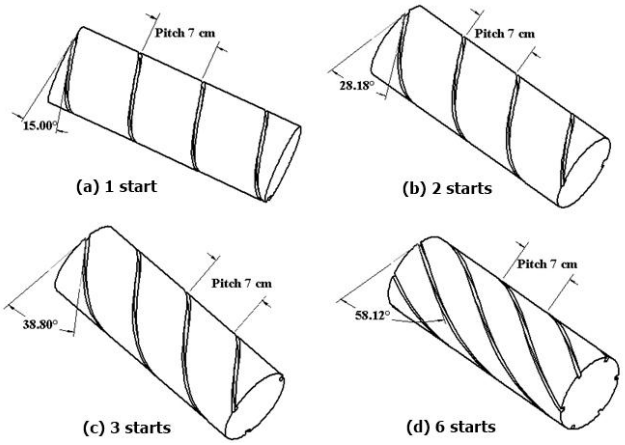

Figure 8- Increasing the angle keeping same pitch ratio and adding required groove start such as (a) single start, 15°, pitch length 7 cm (b) 2 starts, 28°, pitch length 7cm (c) 3 starts, 45°, pitch length 7cm (d) 6 starts, 58°, pitch length 7cm

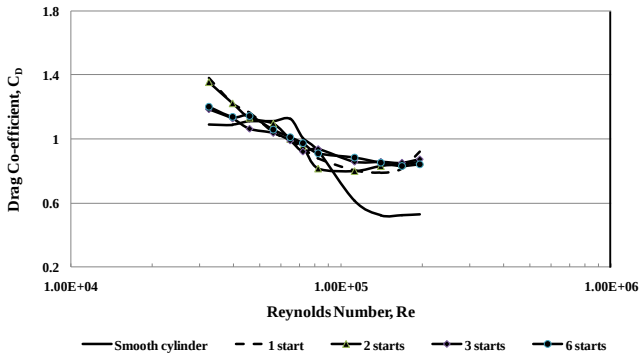

Figure 9. Comparison of these different grooved cylinders with smooth cylinder in drag co-efficient vs Reynolds number

However, among the grooved surfaces, the higher number of starts at low Reynolds number region exhibits lower drag co-efficient but at higher Reynolds number region lower starts number exhibits low drag co-efficient. If it is consider the grooved over the cylinder surface as rough surface, then the roughness increases with the increase of the number of starts. The increase of the groove surface ultimately changes the surface topology which can be resembles to have higher surface roughness. Therefore, one observation from the Figure 9 is that the critical Reynolds number decreases for the increases of the roughness. For example the critical Reynolds number for single start is around 1.4×10^5 and gradually decreases for higher number of starts and for 6 starts the critical Reynolds number is found around 4×10^4. Similar findings are also obtained by Adachi [22] and Hojo [23]. On other hand, comparing the drag forces for different number of starts don't make any significant variation among themselves (see Figure 10). However, upto certain Reynolds number, the values of the drag forces for all the number starts of the grooves and smooth cylinder is almost same. This indicates that the number of starts of the grooves over the cylinder surface play minimum role on drag force when the pitch is remain constant.

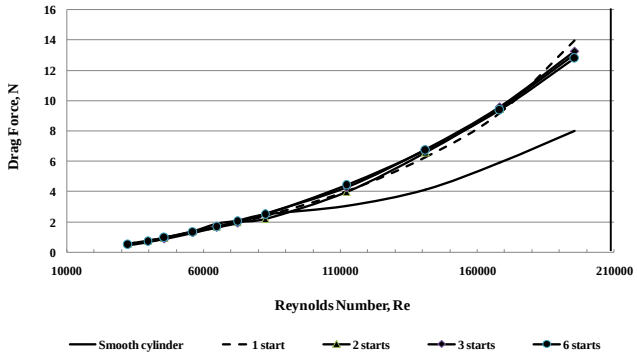

Figure 10. Comparison of drag forces for different Reynolds number for having the same pitch

Variation of Drag by for increasing number of starts:

Experiments are carried out further to investigate the variation of drag coefficient on helical groove over the cylinder surface with increase of the number of start while the groove angle is kept constant which reflects the different pitches with same helical groove. Figure 11 shows the geometrical view of the cylinder with the helical groove for different pitches for the groove angle of 30° for two different numbers of starts like 1 and 2. Figure 12 shows the drag coefficient for the 30° groove angle for two different starts and pitches. The graph shows that the critical Reynolds number for the grooved surface is shifted to a bit lower value as compared with the smooth cylinder and the drag coefficient is much decreased. However, too low Reynolds number exhibits higher drag coefficient which is also for the higher Reynolds number. Comparing the Figure 12 with the Figure 5 and Figure 9, it is evident that number of starts has less contribution on drag coefficient as compared with the pitch of the grooved surface. In fact, Figure 10 reflects that the same pitch with the increase of number of starts don't make any significant influence on drag force. However, comparing the drag forces for different groove angles with different pitches are shown in Figure 13 and indicate that number of starts (also pitches) influences the drag forces. For example, 60° helical angle with six starts resembles to rough surface as compared with 60° helical angle with single start. With this nature of surface exhibits higher drag force as compared with the smooth surface. There is some variation of 30° helical angle with single start which may due to the fault of the wrapped plastic floor and alignment of the edges.

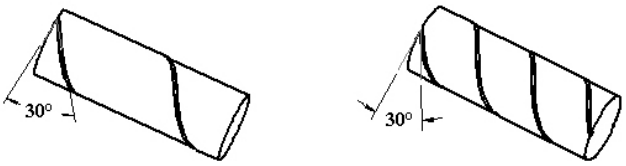

Figure 11. Different pitches with same groove angle of 30°

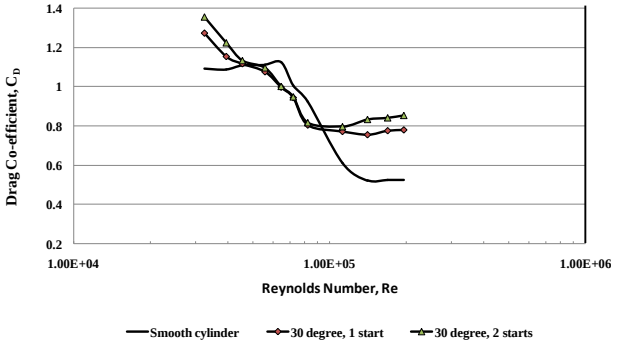

Figure 12. Drag coefficient variation for Reynolds number with 30° groove angle with 1 and 2 starts

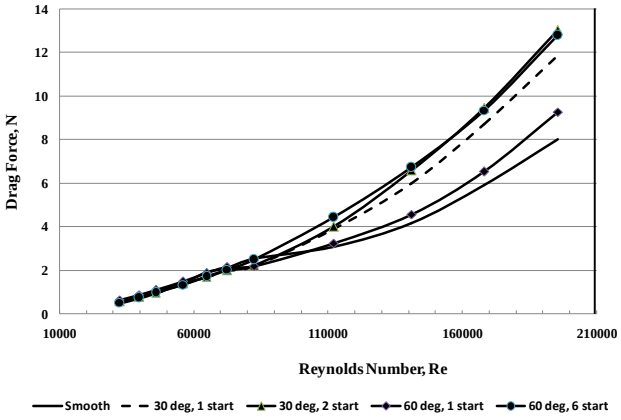

Figure 13. Drag force variation for different Reynolds number

Longitudinal Groove over circular cylinder:

Experimental studies have also been carried out to investigate the drag coefficient for longitudinal groove over the circular cylinder surface. The width and depth of the grooves are maintained same as before.

However, 2 and 4 longitudinal grooves are selected with different orientation across the flow. The calculated drag coefficient from the experimental results are shown in Figure 14 and found that for the higher Reynolds number i.e. super critical Reynolds number the drag coefficient increases and eventually, longitudinally grooves don't make any benefit to drag coefficient. However, for lower Reynolds number i.e. lower than the critical Reynolds number show significant reduction of drag coefficient for the longitudinal grooves as compared with the smooth cylinder. The notation G stands for the number of grooves in longitudinal direction and C stands as Case. Therefore, G4-C1 indicates 4 grooves in longitudinal direction for Case 1. Four different cases with 2 and 4 grooves are considered for drag calculation. For example, drag coefficient for Case G4-C1 has been reduced around 20% of that of smooth cylinder at Reynolds number 8.3×10^4. Huang [19] and Zhou et al. [31] observed the similar amount of reductions on drag coefficient for the cylinder with the longitudinal grooves for the subcritical Reynolds number regions. The Figure 14 also indicates that the position of the groove in the frontal side of the cylinder make differences on the drag coefficient. For the case of helical groove over the circular cylinder and the position of the groove start make significant contribution on flow separation and turbulent wake at the rear end of the cylinder and hence the drag coefficient.

4. Conclusions

Experimental studies on the circular cylinder with helical groove are conducted with different helical groove angle and pitches in subsonic wind tunnel over a wide range of Reynolds number. Results show that the presence of helical groove over the circular cylinder does not improve the drag coefficient for higher Reynolds number. However the results imply that considerable drag coefficient can be reduced at the critical Reynolds number region. In fact, subcritical Reynolds number region is disappeared and drag coefficient gradually decreases with the increase of Reynolds till the critical Reynolds number rather than being straight for the smooth cylinder. Results also show that increasing the number of helical groove starts with the same pitch exhibits higher drag coefficient. However, reducing the pitch over the cylinder surface shows beneficial over the increasing the number of starts. Similar to the helical groove, longitudinal groove also make significant impact on drag coefficient at the critical Reynolds number region and low Reynolds number region.

Acknowledgement

Authors would like to acknowledge the Ahsanullah University of Science and Technology for providing all kind of support.

8. References

1- Sakamoto, H., Tan, K. and Haniu, H., (1991), *An Optimum Suppression of Fluid Forces by Controlling a Shear Layer Separated From a Square Prism*, Journal of Fluids Engineering, Vol.113(2), p.183-189. [DOI: 10.1115/1.2909478]

2- Fujisawa, N. and Takeda, G., (2003), *Flow control around a circular cylinder by internal acoustic excitation*, Journal of Fluids and Structures, Vol.17(7), p.903–913. [DOI: 10.1016/S0889-9746(03)00043-4]

3-Igarashi, T. and Tsutsui, T., (1989), *Flow Control Around a Circular Cylinder by a New Method : 2nd Report, Fluid Forces Acting on the Cylinder*, Transactions of the Japan Society of Mechanical Engineers Series B, Vol.55(511), p.708-714. [DOI: 10.1299/kikaib.55.708]

4- Igarashi, T. and Tsutsui, T., (1991), *Flow Control around a Circular Cylinder by a New Method : 3rd Report, Properties of the Reattachment Jet*,

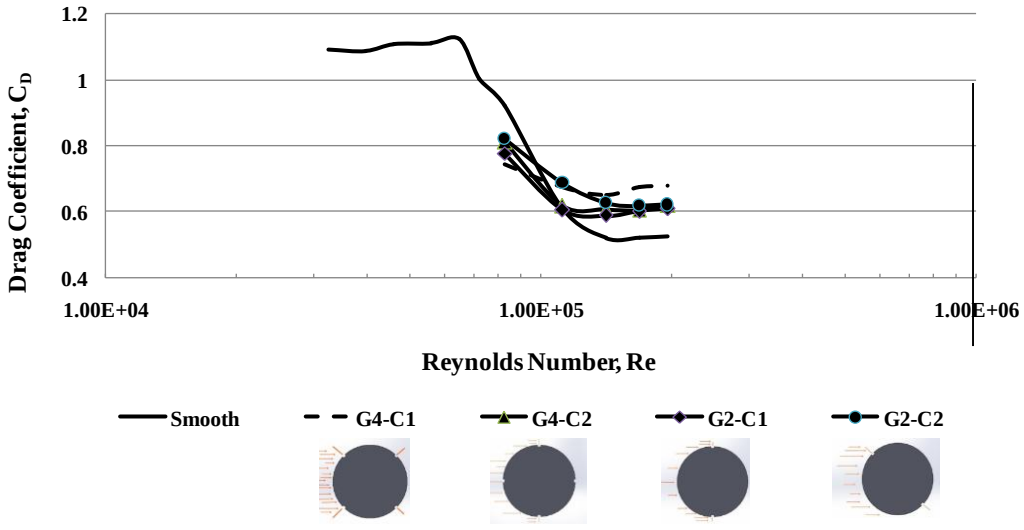

Figure 14. Drag coefficient variation over the Reynolds number for different numbers of longitudinal grooves for different orientation of the cylinder across the flow.

Transactions of the Japan Society of Mechanical Engineers Series B, Vol.57(533), p.8-13. [DOI: 10.1299/kikaib.57.8]

5- Raayai-Ardakani, S. and McKinley, GH., (2017), *Drag reduction using wrinkled surfaces in high Reynolds number laminar boundary layer flows*, Physics of Fluids, Vol.29(093605), p.093605-1-16. [DOI: 10.1063/1.4995566]

6- Matsumoto, H., Kubota, Y., Ohishi, M., and Mochizuki, O., (2016), *Drag on a Cylinder with an Apple-Shaped Cross Section*, World Journal of Mechanics, Vol.6, p.323-339. [DOI: 10.4236/wjm.2016.69024]

7- Yunqing, G., Tao, L., Jiegang, M., Zhengzan, S., and Peijian, Z., (2017), *Analysis of Drag Reduction Methods and Mechanisms of Turbulent*, Applied Bionics and Biomechanics, Article ID 6858720, 8 pages. [DOI: 10.1155/2017/6858720]

8- Zdravkovich, MM., (1977), *Review of Flow Interference Between Two Circular Cylinders in Various Arrangements*, Journal of Fluids Engineering, Vol.99(4), p.618-633.

9- Sakamoto, H. and Haniu, H., (1994), *Optimum Suppression of Fluid Forces Acting on a Circular Cylinder*, Journal of Fluids Engineering, Vol.116(2), p.221-227. [DOI: 10.1115/1.3448871]

10- Bai, Q., Bai, J., Meng, X., Ji, C., and Liang, Y., (2016), *Drag reduction characteristics and flow field analysis of textured Surface*, Friction, Vol.4(2), p.165–175. [DOI: 10.1007/s40544-016-0113-y]

11- Coustols, E., (2001), *Effect of grooved surfaces on the structure of a turbulent boundary layer*, Mec. Ind 2.421-234. Edition scientifique et médicale Elsevier SAS. S1296-2139(01)01125-3/FLA. [DOI: 10.1590/S0100-73862000000100001]

12- Talley, S. and Mungal, G., (2002), *Flow around cactus-shaped cylinders*, Center for Turbulence Research Annual Research Briefs, p.363-376.

13- Yokoi, Y., Igarashi, T. and Hirao, K., (2011), *The Study about Drag Reduction of a Circular Cylinder with Grooves*, Journal of Fluid Science and Technology, 6(4), p.637. [DOI: 10.1590/S0100-73862000000100001]

14- Yamagishi, Y. and Oki, M., (2004), *Effect of Groove Shape on Flow Characteristics around a Circular Cylinder with Grooves*, Journal of Visualization, Vol.7(3), p.209-216. [DOI: 10.1007/BF03181635]

15- Takayama, S. and Aoki, K., (2005), *Flow Characteristics around a Rotating Grooved Circular Cylinder with Grooved of Different Depths*, Journal of Visualization, Vol.8(4), p.295-303. [DOI: 10.1007/BF03181548]

16- Dey, P. and Das, AK., (2015), *Numerical analysis of drag and lift reduction of square cylinder*, Engineering Science and Technology, an International Journal, Vol.18(4), p.758–768. [DOI: 10.1016/j.jestch.2015.05.007]

17- Ranjith, ER., Sunil, AS. and Pauly, L., (2016), *Analysis of flow over a circular cylinder fitted with helical strakes*, International Conference on Emerging Trends in Engineering, Science and Technology (ICETEST-2015), Procedia Technology 24, p.452 – 460. [DOI: 10.1016/j.protcy.2016.05.062]

18- Quen, LK., Abu, A., Kato, N., Muhamad, P., Sahekhaini, A. and Abdullah, H., (2014), *Investigation on the effectiveness of helical strakes in suppressing VIV of flexible riser*, Applied Ocean Research, 44, p.82–91. [DOI: 10.1016/j.apor.2013.11.006]

19- Huang, S., (2011), *VIV suppression of a two-degree-of-freedom circular cylinder and drag reduction of a fixed circular cylinder by the use of helical grooves*, Journal of Fluids and Structures, 27, p.1124–1133. [DOI: 10.1016/j.jfluidstructs.2011.07.005]

20- Fage, A. and Warsap, JH., (1930), ARC R&M1283, (also §191, Modern Developments in Fluid Dynamics. 1965, ed.S. Goldstein).

21- Achenbach, E., (1971), *Influence of surface roughness on the cross-flow around a cylinder*, Journal of Fluid Mechanics, Vol.46(2), p.321-335. [DOI:10.1017/S0022112071000569]

22- Adachi, T., (1995), *The Effect of Surface Roughness of a Body in the High Reynolds Number Flow*, International Journal of Rotating Machinery, Vol.1(3-4), p.187-197. [DOI: 10.1155/S1023621X95000170]

23- Hojo, T., (2015), *Control of flow around a circular cylinder using a patterned surface*, Computational Methods and Experimental Measurements XVII, WIT Transactions on Modelling and Simulation, Vol.59, p.245-256. [DOI: 10.2495/CMEM150221]

24- Rodríguez, I., Lehmkuhl, O., Chiva, J., Borrell, R. and Oliva, A., (2015), *On the flow past a circular cylinder from critical to super-critical Reynolds numbers: Wake topology and vortex shedding*, International Journal of Heat and Fluid Flow, Vol.55, p.91–103. [DOI: 10.1016/j.ijheatfluidflow.2015.05.009]

25- Cengel, YA. and Cimbala, JM., Fluid Mechanics Fundamentals and Applications. McGraw Hill Publishers.

26- Kimura, T. and Tsutahara, M., (1991), *Fluid dynamic effects of grooves on circular cylinder surface*, AIAA Journal, Vol.29 (12), p.2062-2068. [DOI: 10.2514/3.10842]

27- Sumer, BM. and Fredose, J., (1997), *Hydrodynamics around circular cylinder*, Vol.12, World Scientific publishing Co. Pte. Ltd.

28- Alonzo-García,A., Gutiérrez-Torres, C.del C. and Jiménez-Bernal, JA., (2014), *Large Eddy Simulation of the Subcritical Flow over a U-Grooved Circular Cylinder*, Advances in Mechanical Engineering, Vol.2014, Article ID 418398, 14 pages. [DOI: 10.1155/2014/418398]

29- Nakamura, Y. and Tomonari, Y., (1982), *The effects of surface roughness on the flow past circular cylinders at high Reynolds numbers*, Journal of Fluid Mechanics, Vol.123, p.363–378. [DOI: 10.1017/S0022112082003103]

30- Ko, NWM., Leung, YC. and Chen, JJJ., (1987), *Flow past V-groove circular cylinders*, AIAA journal, Vol.25(6), p.806–811. [DOI: 10.2514/3.9704]

31- Zhou, B., Wang, X., Guo, W., Zheng, J., Tan, SK., (2015), *Experimental measurements of the drag force and the near-wake flow patterns of a longitudinally grooved cylinder*, Journal of Wind Engineering and Industrial Aerodynamics , Vol.145, p.30–41. [DOI: 10.1016/j.jweia.2015.05.013]